

SAR Imagery of Boquerón Bay Fault (NBBF)

CORAL ROIG- SILVA

Department of Geology

University of Puerto Rico

P.O. Box 9017, Mayaguez, Puerto Rico 00681-9017

Email: crs9142@uprm.edu

ABSTRACT

In these work we investigate the modules provided in ENVI for the analysis of SAR images. We used two types of images; one was a TIFF formatted image (a representation of a SAR image) and the other a CEOS formatted image (data acquired from SAR in Radarsat-1). From the information obtained we concluded that Local sigma and bit error adaptive filters suits best to preserve detail, and that morphology filters mark with a change in gray scale a line in the location of the NBBF area.

KEYWORDS: Radarsat-1, SAR, ENVI, Puerto Rico, lineaments

INTRODUCTION

Synthetic Aperture Radar (SAR) imagery has being used extensively in the geosciences to serve different purposes; it has being used to study active volcanoes in tropical regions, flooding during extensive rainfall, to identify lineaments¹, and so forth (Bonn, F., and Dixon, R., 2005; Carn, S.A., 1999; Catani, F. et al, 2004; Fielding, E.J et al, 1998; Fielding, E.J et al 2004; Majumdar, T.J., and Massonet, D., 2002; Paradella, W.R. et al 2000; Tralli, D.M. et al 2005; Weydahl, D.J. et al., 2004; Wicks, C.W. et al. 2001). Ideally, SAR imagery gives us information about the surface moisture, roughness and topography. In this paper we use the topography enhancement advantage of SAR imagery to try to identify any lineament that might be related to faults.

MATERIALS AND METHODS

¹ The term lineament is used in this paper to refer to any linear feature observed in an image that might be or might not be related to fault escarpments.

We used SAR imagery obtained from RADARSAT-1 acquired on December 8, 1999, taken with a standard 3-beam mode, giving a spatial resolution of 25m. We apply different filters to a TIFF image (Figure 1) to establish what filters will suit our purposes and later apply these filters to the RADARSAT imagery (Figure 1). We used the Environment for the Visualizing Images (ENVI) program, developed by Research System Inc. to process these images and to apply these filters.

Study area

The Lajas valley is a 30 km long, 1.5- 9.0 km wide, E-W trending linear depression bounded at the north and at the south by abrupt mountains. It is characterized by a close drainage formed by the Laguna Cartagena, Laguna de Guánica, and Ciénaga El Anegado (Figure 3). Because of this linear orientation and closed drainage pattern it has being suggested that the valley is controlled by faults, but there was no evidence to prove that faulting occurred onshore western Puerto Rico.

Recent studies (Prentice, C.S. and Mann, P. 2005) have demonstrated that surface rupture occurred during the Holocene occurring in previously unrecognized, unmapped faults along an alluvial fan in southern Lajas Valley. Meanwhile, existing multi-channel seismic profile offshore Puerto Rico (PR), collected by Western Geophysical in 1972, was re-analyzed by Ocasio (2004) identifying a fault at the north of the Boquerón Bay. Ocasio (2004) suggested that this fault extended but the only evidence presented in her work was a Landsat image with what appeared to be a displaced stream. Later, that same year, Roig (2004) used Multi-channel Analysis of Surface Waves to corroborate that the fault extends onshore.

OBJECTIVES

The main scopes in this paper is to present the different features and modules that ENVI provides to the analysis of SAR imagery, and apply these analysis to a geological point of view, in this case, the identification of lineaments. After understanding the modules provided by ENVI, we apply different filters and analysis to the images and try to make an analysis of the images on the basis of geomorphology and lineaments.

RESULTS AND DISCUSSIONS

We first explored the different modules and filters that ENVI have to analyze radar data using the TIFF image of a SAR image of southwestern Puerto Rico. First we applied all adaptive filters available in ENVI, we applied texture filters, convolution filters and then morphological filters. After applying these filters we determined which filter best suits our purpose best, and then apply it to the RADARSAT-1 SAR image of the area of Boquerón.

Adaptive Filters

An adaptive filter uses a standard deviation of those pixels within a box surrounding each pixel to calculate a new pixel value. Usually the original value is replaced to the one calculates (those that satisfy the standard deviation criteria). Adaptive filters preserve image sharpness and detail while suppressing noise (speckle). Applying these filters resulted in the lost in detail using some filters (Figure 4). These differences might be due to the nature of the image as is not a SAR data image per se. Is important to observe that these filters, although they change the pixel values, they preserve the pixel behavior, meaning that if a pixel has a higher value (brighter) than other pixel (lower) this relationship will prevail.

Lee-These filters is used to smooth noisy (speckle) data that have an intensity related to the image scene and that also have a multiplicative and/or additive component. Lee filter is a standard deviation base (sigma) filter that filters database on statistics calculated within individual filter windows. The pixel being filtered is replaced by a value calculated using the surrounding pixels. (Figure)

Enhanced Lee-Is a variation of Lee filters and similarly uses local statistics (coefficient variation) within individual filter windows. Each pixel is put into one of three classes: homogeneous (the pixel value is replaced by the average of the filter window),

heterogeneous (the pixel value is replaced by a weighted average), or target point (where the pixel value is not changed). Each type of class is treated differently.

Frost-Is an exponentially damped circularly symmetric filter that uses local statistics. The pixel value is replaced with a value calculated based on the distance from the filter center, the damping factor, and the local variance.

Enhanced frost-Variation of the Frost filter uses the same statistic as the enhanced lee, meaning the uses the coefficient variation to assign each pixel to a class (homogeneous, heterogeneous, or target point). These classes having the same effect on the pixel value as in the enhanced Lee filter.

Kuan-It transforms the multiplicative noise model into an additive noise model. Similar to the Lee, but uses a different weighting function. Again, the pixel value is replaced by a value based on local statistics.

Gamma-Similar to Kuan filter, but it assumes that the values of the pixels are gamma distributed.

Localized Sigma-Uses local standard deviation computed for the filter box to determine valid pixels within the filter window. It replaces the pixel value with the mean calculated using only the valid pixels within the box.

Bit error-Uses an adaptive filter to replace spike pixels with the average of neighboring pixels. He local statistics (mean and standard deviation) within the filter box are used to set a threshold for valid pixels.

Texture Filters

Many images contain regions characterized by variation in brightness rather than any unique value of brightness. Texture refers to the spatial variation of image tone as a

function of scale. To be defined as a distinct textural area, the gray levels within the area must most be more homogeneous as a unit than areas having different textures.

Occurrence Filters

ENVI provides five different texture filters that are based on occurrence measures. These filters are: data range, mean, variance, entropy, and skewness. Occurrence uses the occurrence of each gray level within the processing window for the texture calculation. (Figure 5)

Co- occurrence Filters

These filters are based on the co-occurrence matrix. These include mean, variance, homogeneity, contrast, dissimilarity, entropy, second moment, and correlation. Co- occurrence measures use gray- tone spatial dependence matrix to calculate texture values. This is a matrix of relative frequencies with which pixel values occurs in two neighboring processing windows separated by a specified distance and direction. It shows the number of occurrences of the relationship between a pixel and its specified neighbor. (Figure 6)

Convolution Filters

Convolution filters produce images in which the brightness value at a given pixel is a function of some weighted average of the brightness of the surrounding pixels. Convolution of a user-selected kernel with the image array returns a new, spatially filtered image. In ENVI, we can select the kernel size and values to generate different types of filters. Standard filters include high pass, low pass, Laplacian, directional, Gaussian, median, Sobel, Roberts, and user-defined.

Laplacian

A Laplacian filter is a second derivative edge enhancement filter that operates without regard to edge direction. Laplacian filtering emphasizes maximum values within the image by using a kernel with a high central value typically surrounded by negative weights in the north-south and east-west directions and zero values at the kernel corners.

ENVI's default Laplacian filter uses a 3 x 3 kernel with a value of 4 for the center pixel and values of -1 for the north-south and east-west pixels. All Laplacian filters must have odd kernel sizes. (Figure 7)

Directional

A directional filter is a first derivative edge enhancement filter that selectively enhances image features having specific direction components (gradients), in this case we used an arbitrary- selected angle number of 35 degrees. The sum of the directional filter kernel elements is zero. The result is that areas with uniform pixel values are zeroed in the image, while those that are variable are presented as bright edges. (Figure 8)

Morphology Filters

Morphology filter are mathematical morphology filtering that are a non-linear method of processing digital images on the basis of shape. Its primary goal is the quantification of geometrical structures.

Dilate

Dilate filters; commonly known as fill, expand, or grow, fills holes smaller than the structural element (kernel) in a binary or gray scale image. (Figure 9)

Closing

Closing filters smooth the contours, fuse narrow breaks and long thin gulfs, eliminate small holes, and fill gaps in the contours of an image. The closing of an image is defined as the dilation of the image followed by subsequent erosion using the same structural element. (Figure 10).

RADARSAT-1 image data

The first important step to analyze the SAR image data obtained form RADARSAT -1 was the antenna pattern correction; this correction is necessarily to correct any wrong signal that may be due to the geometry of the image and the travel of the signal. (Figure 11)

After applying these corrections, we apply adaptive filters (Lee, Enhanced lee, Local sigma and bit error). (Figure 12) Then we applied texture filters (figure 13 and figure 14), convolution (figure 15 and figure 16) and morphology filters (figure 17 and figure 18).

CONCLUSIONS

From our work we believe that the best adaptive filter that suits the investigation of faults and lineaments are the local sigma and the bit error, since they preserve fine detail that it is lost with the other adaptive filters. The textures filters serve well in the determination of which of the adaptive filters preserve detail.

Convolution filters serve us to observe differences in brightness between pixels. In the TIFF image, the morphology filters marked a line, marked by changes in the gray scale, in the more or less exact location where the North of Boquerón Bay Fault is located, this can be seeing after applying any of the dilate or closing morphology filters. It's important to remember that this was one of many steps before analyzing an image. In this case, it has being somewhat complicates because of the nature of the image and the time we had to make interpretations. In the future we expect to analyze better and more the SAR image taken with Radarsat-1 so we can obtain further information about the topography of the area that may lead to the identification of lineaments that as well might be related to faulting in the area and may represent a seismic hazard for the area.

REFERENCES

Bonn, F., and Dixon, R. 2005. Monitoring Flood Extend and Forecasting Excess Runoff Risk with RADARSAT- Data. Natural Hazards. V. 35. Pp. 377- 393

Cameron- Gonzalez, Antonio E. 2004. Landsat TM processing in the investigation of active fault zones, South Lajas Valley Fault Zone and Cerro Goden Fault Zone as an example. Geol 6225: Advance Remote Sensing Class.

Carn, S.A. 1999. Application of synthetic aperture radar (SAR) imagery to a volcano mapping in the humid tropics: a case study in East Java, Indonesia. *Bull Volcanol.* V. 61. Pp. 92- 105

Catani, F., Farina, P., Moretti, S., Nico, G., and Strozzi, T. 2004. On the application of SAR interferometry to geomorphological studies: estimation of landform attributes and mass movements. Doi: 10.1016/j.geomorph.2004.08.012

Fielding, E.J., Blom, R.G., and Goldstein, R.M. 1998. Rapid subsidence over oil fields measured by SAR interferometry. *Geophysical Research Letters.* V. 25. Pp. 3215-3218

Fielding, E.J., Wrigth, T.J., Muller, J., Parsons, B.E., and Walker, R. 2004. Aseismic deformation on a fold-and- thrust belt imaged by synthetic aperture radar interferometry near Shahdad, southeast Iran. *Geology.* V. 32. No.7.Pp. 577- 580

Majumdar, T.J., and Massonet, D. 2002. D-InSAR applications for monitoring of geological hazards with special reference to Latur earthquake 1993. *Current Science.* V.83. No. 4. Pp. 502-508

Paradella, W.R., Dos Santos, A.R., Veneziani, P., and De Moraes, M.C. 2000. Synthetic Aperture Radar for Geological Applications in the Moist Tropics: Experiences from the Brazilian Amazon Region. *Revista Brasileira de Geociências.* V. 30. No. 3. Pp. 538- 542

Prentice, C.S., and Mann, P. 2005. Paleoseismic study of the South Lajas Fault: First documentation of an onshore Holocene fault in Puerto Rico. Mann, P. ,ed. *Active tectonics and seismic hazards of Puerto Rico, the Virgin Islands, and onshore areas: Geological Society of America Special Paper 385.* Pp. 215-222.

Ocasio Campos, D.M. 2004. An onshore total intensity magnetic study of Boquerón Bay area, Southwestern Puerto Rico. Undergraduate research, University of Puerto Rico, Mayagüez Campus.

Roig Silva, Coral. 2004. Multi-channel Analysis of Surface Waves to map the North Boquerón Bay Fault. Undergraduate research, University of Puerto Rico, Mayagüez Campus.

Tralli, D.M., Blom, R.G., Zlotnicki, V., Donnellan, A., and Evans, D.L. 2005. Satellite remote sensing of earthquake, volcano, flood, landslide and coastal inundation hazards. ISPRS Journal of Photogrammetry & Remote Sensing. V. 59. Pp. 185- 198.

Weydahl, D.J., Bretar, F., and Bjerke, P. 2004. Comparison of RADARSAT-1 and IKONOS satellite images for urban features detection. Doi: 10.1016/j.inffus.2004.07.001

Wicks, C.W., Thatcher, W. Monastero, F.C., and Hasting, M.A. 2001. Steady- State Deformation of the Cabo Range, East- Central California, Infrared from Satellite Radar Interferometry

FIGURES

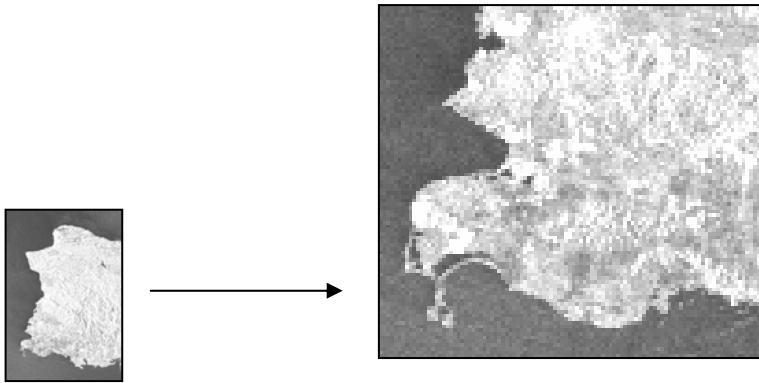


Figure 1: Tiff image from a SAR image. Cropped to enhance the area of the Lajas valley.

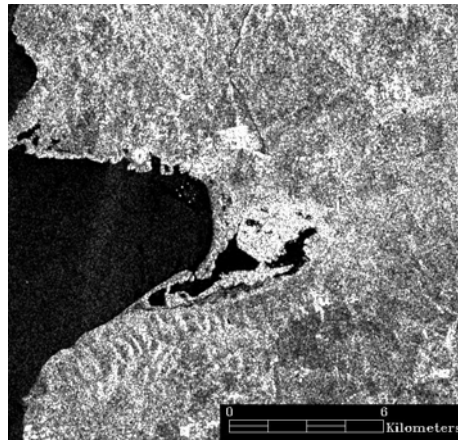


Figure 2: Cropped image of the RADARSAT-1 data for southwestern Puerto Rico.



Figure 3: Geographic location of the study area, Boquerón, Cabo Rojo, Puerto Rico.

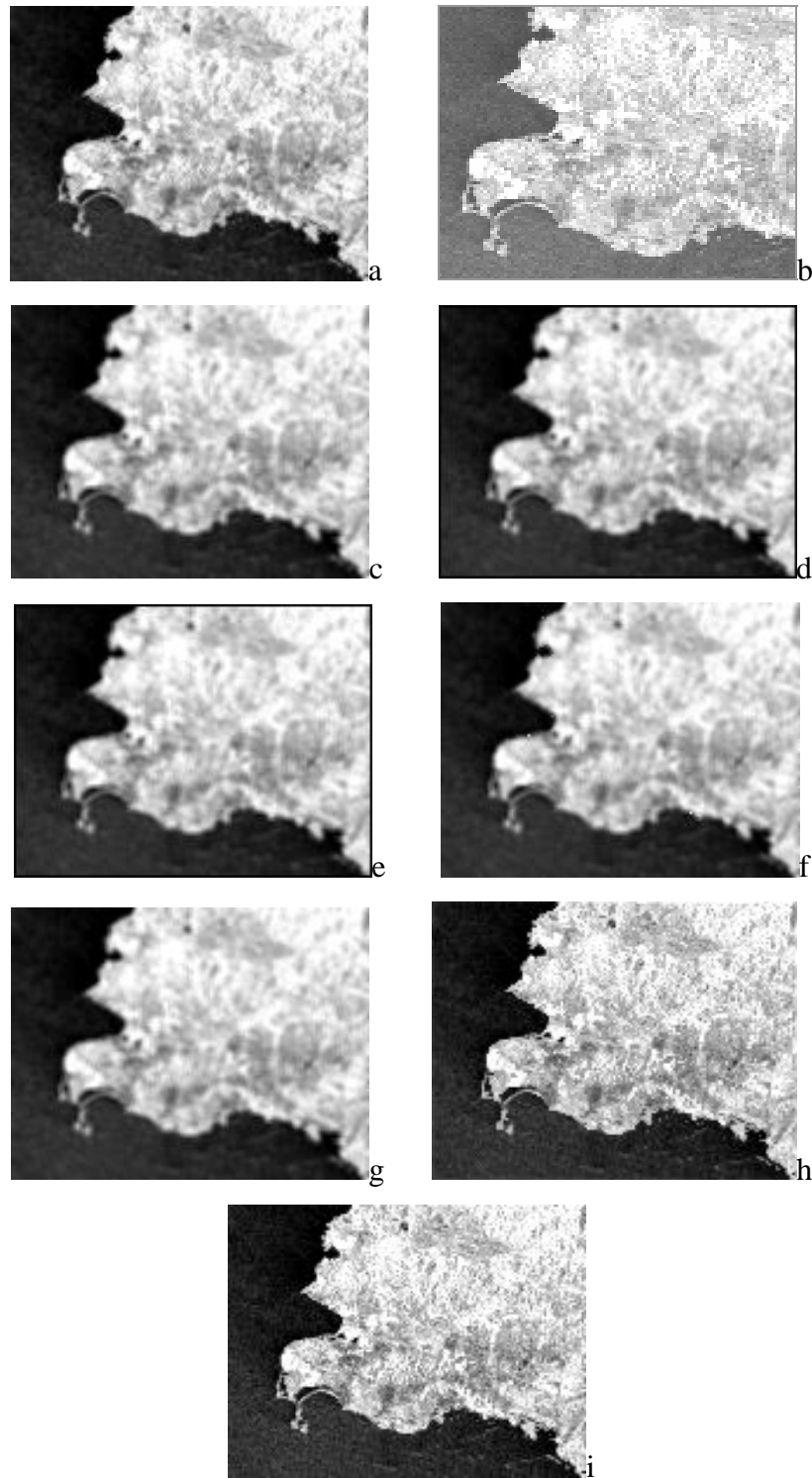


Figure 4: Adaptive filters applied to the TIFF image of a SAR image: a) Image without filter, b) Lee filter, c) Enhanced Lee, d) Frost, e) Enhanced frost, f) Kuan, g) Gamma, h) Localized Sigma, and i) Bit Error. See text for explanation.

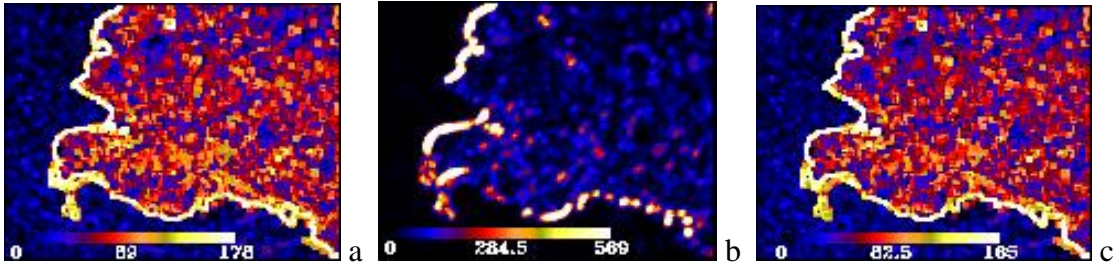


Figure 5: Texture filters- Occurrence filter, Data Range; occurrence filter applied to different images with and without adaptive filters, a) No adaptive filter, b) Enhanced Lee, c) Localized Sigma.

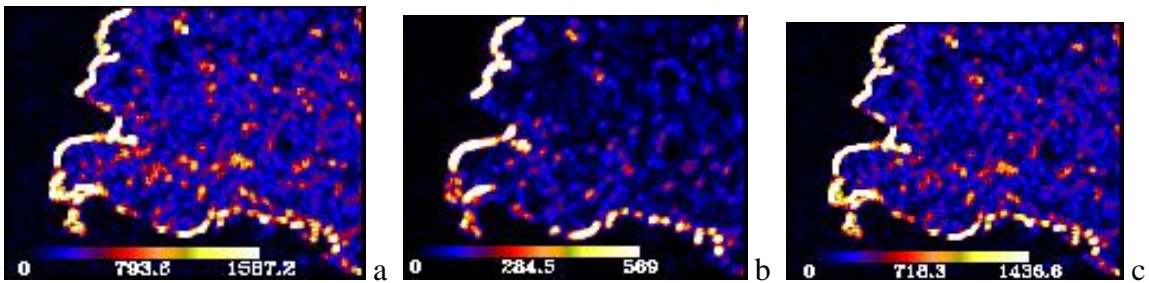


Figure 6: Co-occurrence filters, contrast, Data Range; co- occurrence filters applied to different images with and without adaptive filters, a) no adaptive filter, b) enhanced lee, c) localized sigma.

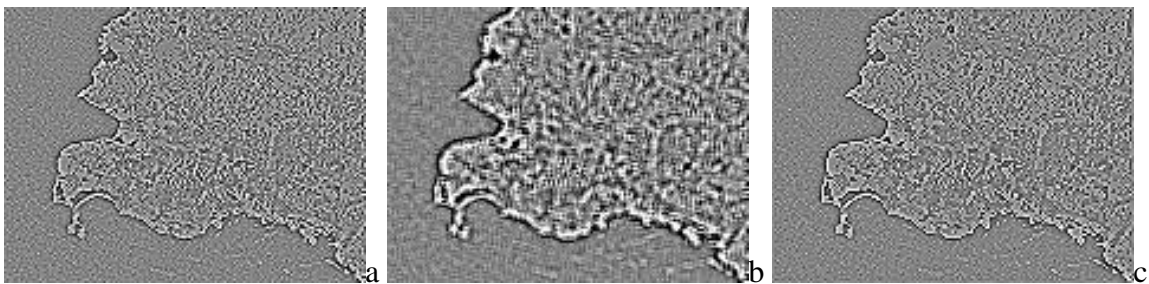


Figure 7: Convolution Filters, Laplacian; applied to different images with or without adaptive filters, a) no adaptive filter, b) enhanced lee, c) localized sigma.

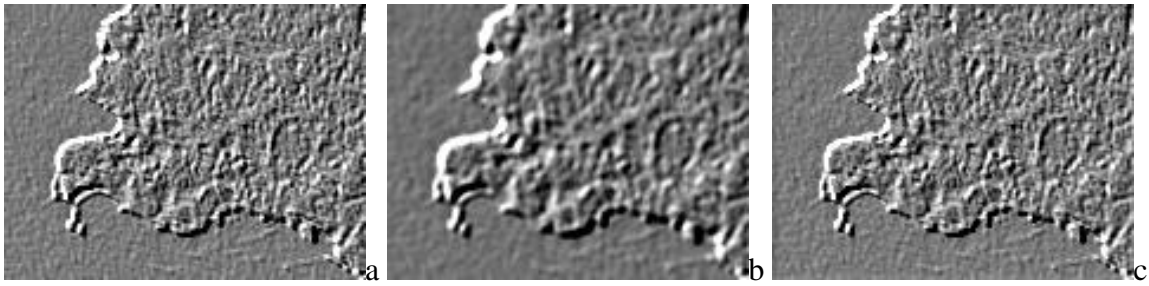


Figure 8: Convolution filters, Direct; applied to different images with or without adaptive filters using an angle of 35 degrees, a) no adaptive filter, b) enhanced lee, c) localized sigma.

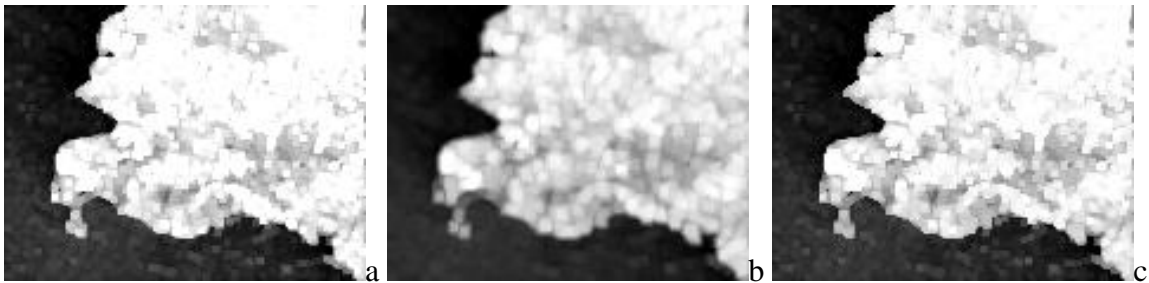


Figure 9: Morphology filters, Dilate; applied to different images with or without adaptive filters, a) no adaptive filter, b) enhanced lee, c) localized sigma.

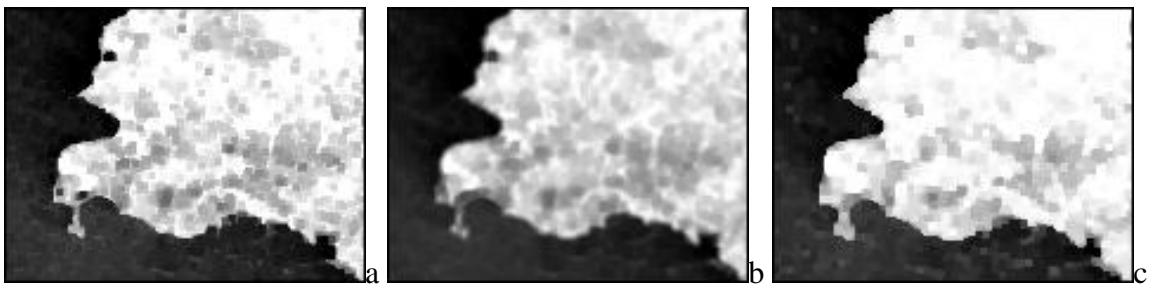


Figure 10: Morphology filters, Closing; applied to different images with or without adaptive filters, a) no adaptive filter, b) enhanced lee, c) localized sigma.

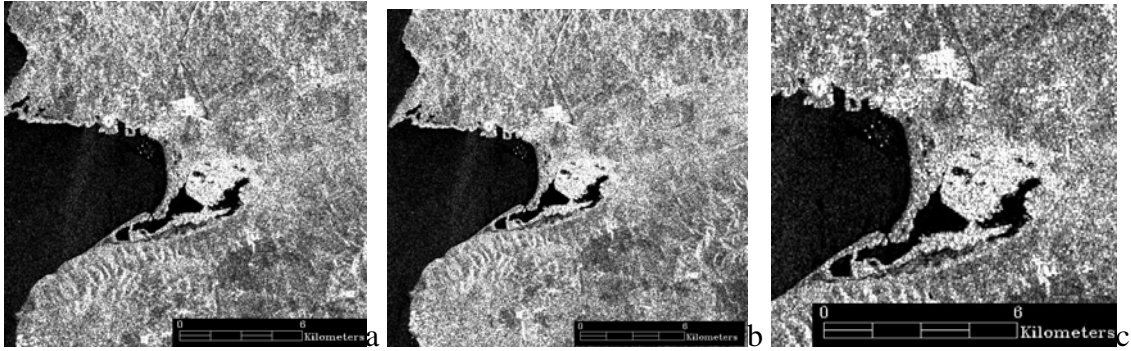


Figure 11: RADARSAR-1 image; a) image without antenna pattern calibration (APC), b) APC1 multiplicative, c) APC2 additive.

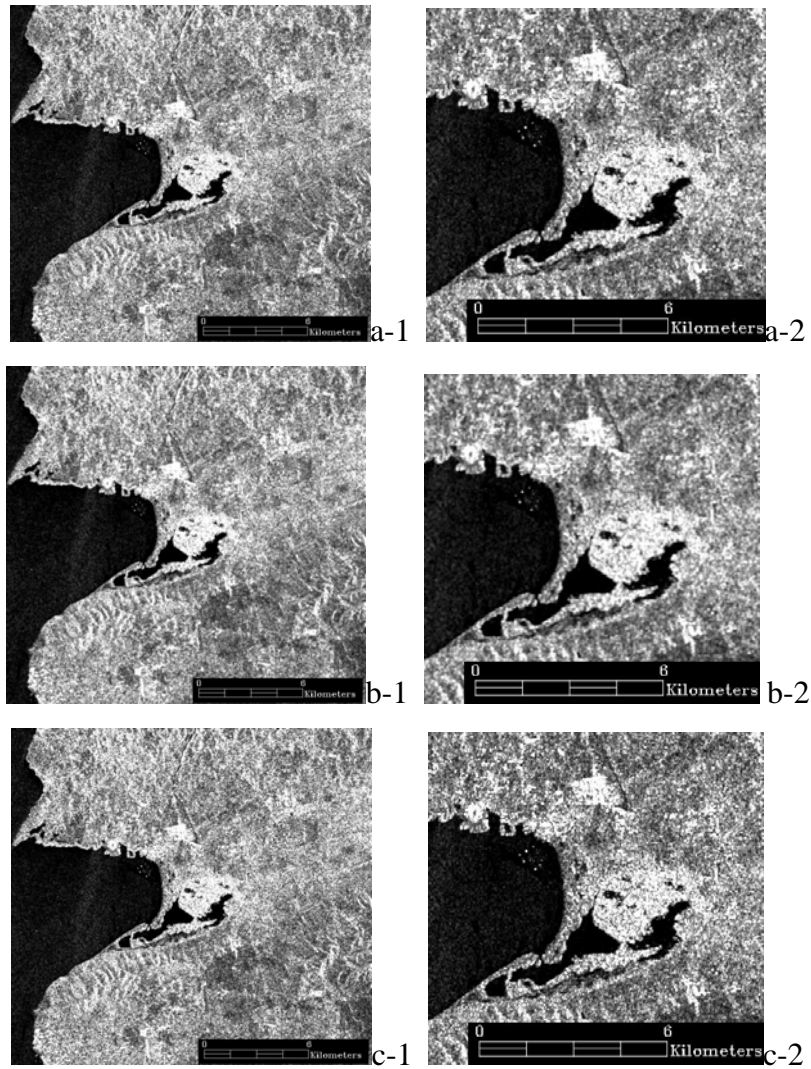


Figure 12: Radarsat-1 image data, adaptive filters; a) Lee filters (a-1 ACP1, a-2 ACP2), b) Enhanced Lee (a-1 ACP1, a-2 ACP2), c) Bit error (a-1 ACP1, a-2 ACP2)

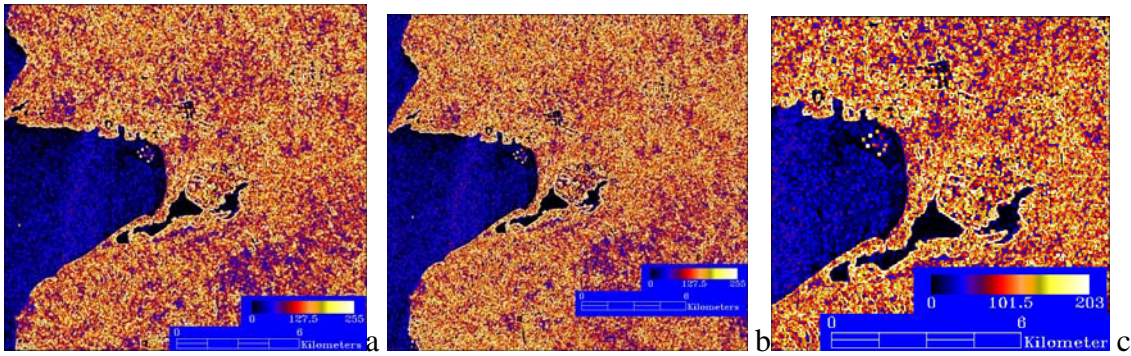


Figure 13: Radarsat-1 image data, texture filters, occurrence data range; a) image without ACP, b) image with ACP1, c) image with ACP2

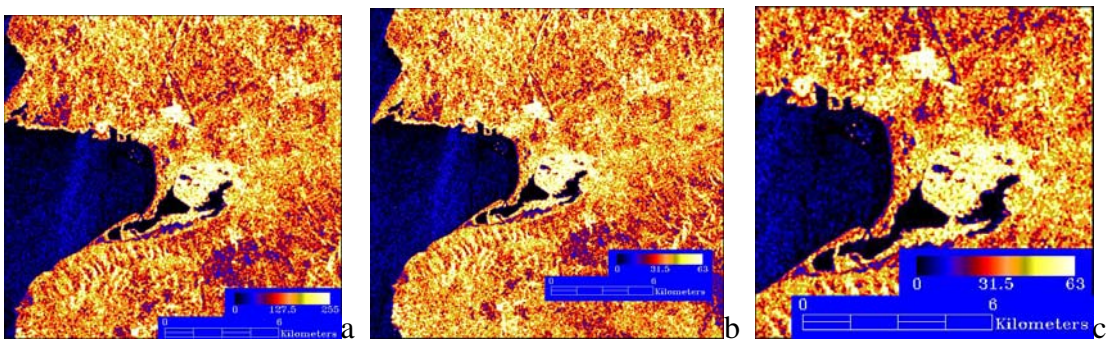


Figure 14: Radarsat-1 images, texture filters, co-occurrence contrast; a) image without ACP, b) image with ACP1, c) image with ACP2

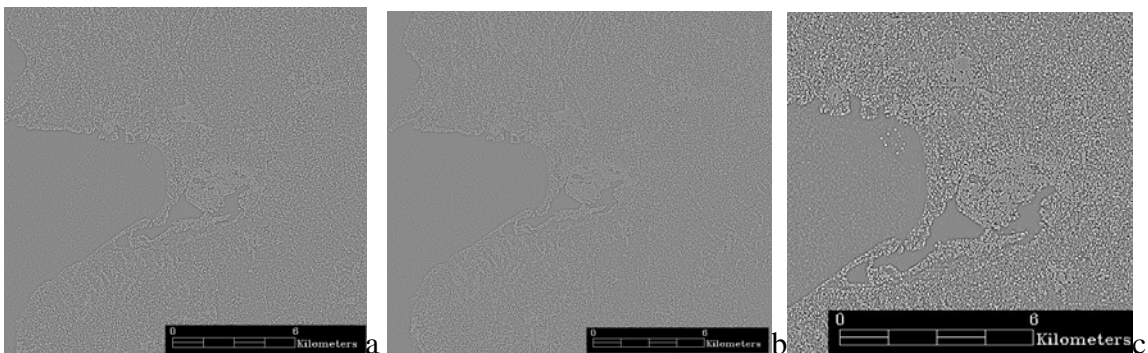


Figure 15: Radarsat-1 image, Convolution filters, Laplacian; a) image without ACP, b) image with ACP1, c) image with ACP2

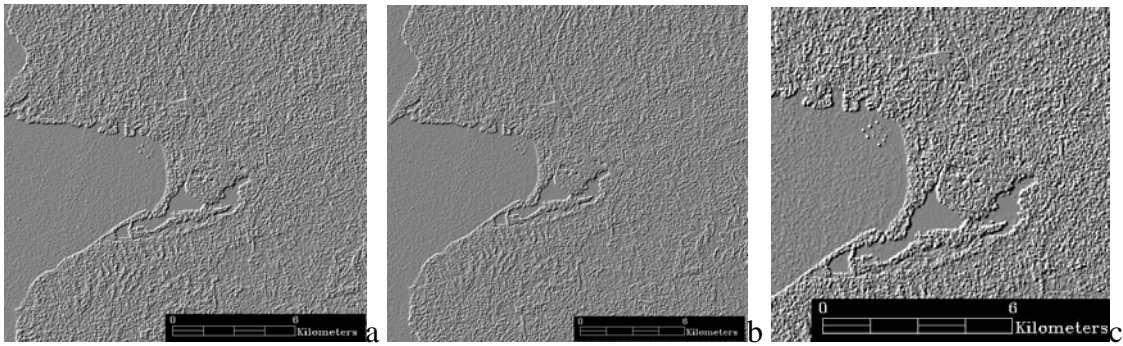


Figure 16: Radarsat-1 image, Convolution filters, Direct at an angle of 35 degrees; a) image without ACP, b) image with ACP1, c) image with ACP2

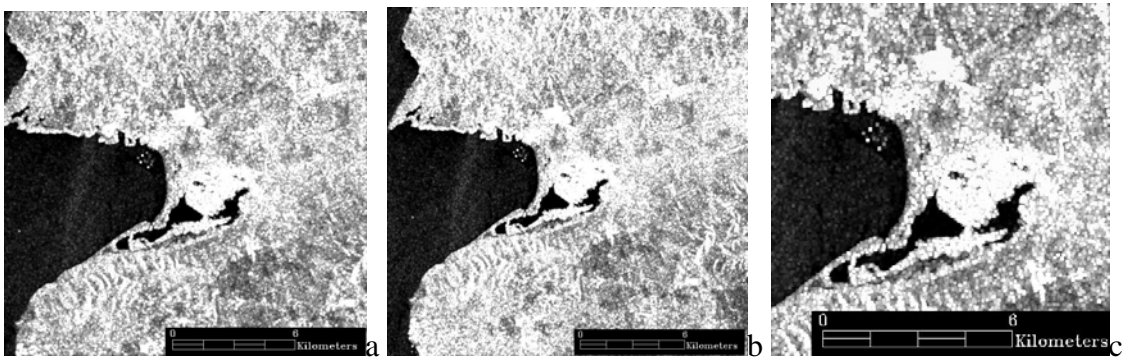


Figure 17: Radarsat-1 image, Morphology filter, Dilate; a) image without ACP, b) image with ACP1, c) image with ACP2

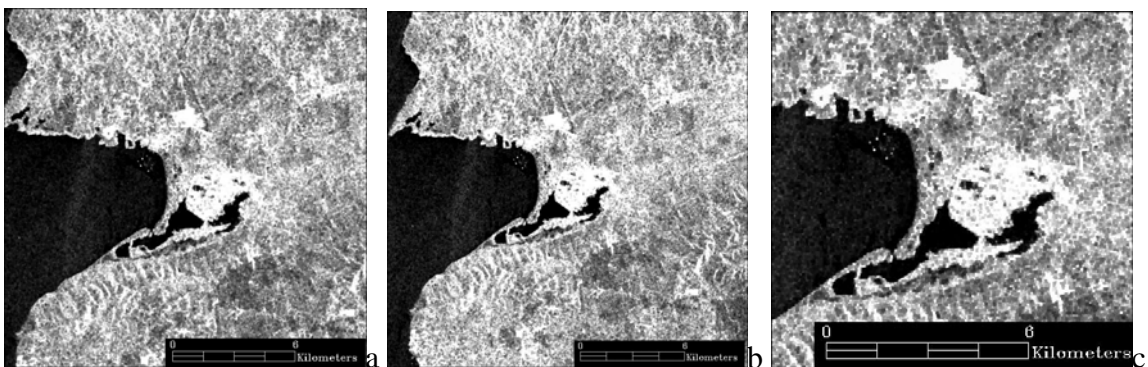


Figure 18: Radarsat-1 image, Morphology filter, Closing; a) image without ACP, b) image with ACP1, c) image with ACP2